

# A hyper-runaway white dwarf in *Gaia* DR2 as a Type Ia supernova primary remnant candidate

Nicholas J. Ruffini<sup>1</sup>\* & Andrew R. Casey<sup>1,2</sup>

<sup>1</sup>*School of Physics and Astronomy, Monash University, Victoria 3800, Australia*

<sup>2</sup>*Faculty of Information Technology, Monash University, Victoria 3800, Australia*

Accepted 2019 July 30. Received 2019 July 26; in original form 2018 October 17.

## ABSTRACT

Observations of stellar remnants linked to Type Ia and Type Ia supernovae are necessary to fully understand their progenitors. Multiple progenitor scenarios predict a population of kicked donor remnants and partially-burnt primary remnants, both moving with relatively high velocity. But only a handful of examples consistent with these two predicted populations have been observed. Here we report the likely first known example of an unbound white dwarf that is consistent with being the fully-cooled primary remnant to a Type Ia supernova. The candidate, LP 93-21, is travelling with a galactocentric velocity of  $v_{\text{gal}} \simeq 605 \text{ km s}^{-1}$ , and is gravitationally unbound to the Milky Way. We rule out an extragalactic origin. The Type Ia supernova ejection scenario is consistent with its peculiar unbound trajectory, given anomalous elemental abundances are detected in its photosphere via spectroscopic follow-up. This discovery reflects recent models that suggest stellar ejections likely occur often. Unfortunately the intrinsic faintness of white dwarfs, and the uncertainty associated with their direct progenitor systems, makes it difficult to detect and confirm such donors.

**Key words:** white dwarfs – stars: kinematics and dynamics

## 1 INTRODUCTION

Type Ia supernovae (SNe Ia) are the thermonuclear explosions of carbon-oxygen (C/O) white dwarfs (WDs) (Iben & Tutukov 1984; Nomoto 1982). SNe Ia have been used to calibrate cosmological distance scales (Nomoto et al. 1997; Perlmutter et al. 1999) and cosmological models (Riess et al. 1998), yet our knowledge on the progenitors of SNe Ia remains incomplete. Although the precise progenitor system is unknown, it is generally accepted a primary WD is stimulated via mass accretion from, or merges with, a companion to explode as a SN Ia (Wang & Han 2012).

In the so-called “single-degenerate” (SD) scenario (Whelan & Iben 1973; Nomoto 1982), the companion is a non-degenerate hydrogen- or helium-star (H-star and He-star, respectively) which donates material from its outer layers to the primary, mass-accreting WD. In the “double-degenerate” (DD) scenario (Iben & Tutukov 1984; Webbink 1984), the donating companion is another WD. A merger is possible in either scenario. Whether or not a primary WD and companion star will lead to the SD or DD scenario depends on parameters such as the initial masses of the components, their separation, and metallicity (Iben & Tutukov 1994; Wang & Han 2010). These parameters also determine which of the

many sub-channels each scenario will likely take (Wang & Han 2011; Liu et al. 2018).

The explosion of the primary WD can be triggered multiple ways in either scenario (Iben & Tutukov 1984; Webbink 1984; Pakmor et al. 2012; Seitzzahl et al. 2013; Papish et al. 2015; Shen et al. 2018b). Theory and observations both suggest different combinations of triggering mechanisms may describe various observed abundance patterns in SN Ia remnants (Seitzzahl et al. 2013; Fink et al. 2014). This implies that both near-Chandrasekhar (near-Ch) mass WDs and sub-Chandrasekhar (sub-Ch) mass WDs, either in the SD or DD scenario, explode to contribute to all observed SNe Ia.

Recent models suggest that the donor will almost always survive the explosion (Pan et al. 2012a; Shen et al. 2018a; Liu et al. 2018). In cases of complete primary WD detonation, the surviving companion will be kicked away with a velocity roughly equal to the binary’s pre-explosion orbital velocity (Eldridge et al. 2011; Wang & Han 2011). This population of kicked non-degenerate/degenerate stars should show evidence of the SN Ia in their photosphere (Pan et al. 2012a,c; Shen & Schwab 2017; Shen et al. 2018a; Tanikawa et al. 2018). Regardless of the evolutionary stage of the kicked donor, it will ultimately evolve to the main WD cooling sequence (Hansen 2003; Justham et al. 2009). Therefore a population of kicked WDs are expected from the

\* E-mail: nick.ruffini@monash.edu

SN Ia scenario, harbouring evidence of their close proximity to thermonuclear supernova. We denote this entire kicked WD population as donor remnants (DRs) regardless of their evolutionary phase during the progenitor stage.

It has also been suggested that the primary WD can survive its own failed detonation in a sub-luminous SN Iax event (Foley et al. 2013; Kromer et al. 2013). If the primary WD remains intact, the asymmetry in the partial deflagration could lead to its ejection from the binary and tell-tale ashes may remain visible in its photosphere (Jordan et al. 2012). It has also been argued that the partial deflagration does not warrant an ejection of the companion (Kromer et al. 2013; Fink et al. 2014). In either case, the possibly intact primary WD is a different kind of remnant – one that should show evidence of the sub-luminous SN Iax in their own photosphere. These “primary remnants” (PRs) should also eventually fall to the main WD cooling sequence (Jordan et al. 2012; Kromer et al. 2013; Zhang et al. 2019).

LP 93-21<sup>1</sup> is a single, DQ spectral-type WD, known since 1976 to have strong carbon Swan Bands and a peculiarly high proper motion (Luyten 1976). In this paper, we examine the properties of LP 93-21 and argue that it is an evolved PR which was kicked to its abnormally high space velocity by its own partial deflagration. We also discuss the possibility that LP 93-21 may also be an evolved donor. In Section 2, we present recent observational data and atmospheric analysis of LP 93-21 to provide updated estimates of its total space motion, mass, age, and origin. In Section 3, we analyse the kinematics of LP 93-21 in context with these updated estimates and assess the viability of the SNe Ia/Iax progenitor scenario. We conclude in Section 4.

## 2 OBSERVATIONS

Here we report on the most up-to-date observations and parameter estimates of LP 93-21. LP 93-21 was first examined in detail by Greenstein et al. (1977) as a carbon degenerate. Its spectrum showed particularly strong C<sub>2</sub> molecular bands, and its proper motion made it a high-velocity WD. The Sloan Digital Sky Survey (SDSS) has spectroscopic confirmation of over nineteen-thousand white dwarfs, most with reported radial velocities (Kleinman et al. 2013; Blanton et al. 2017; Abolfathi et al. 2018). The European Space Agency’s *Gaia* satellite has also observed over twenty-five thousand white dwarfs, measuring their proper motion and parallax with milliarcsecond accuracy (Gaia Collaboration et al. 2016; Lindegren et al. 2018; Gaia Collaboration et al. 2018). Both surveys have since re-observed LP 93-21, providing improved measurements which confirm both its peculiarly fast motion and strong carbon spectral features.

### 2.1 Kinematics

The high precision of *Gaia* DR2 measurements (see Table 1) for LP 93-21 provide a parallax measurement of  $\varpi = 17.48 \pm$

<sup>1</sup> Also known as LHS 291 (Luyten 1976), EGGR 434 (Greenstein et al. 1977), WD 1042+593 and WD 1042+59 (McCook & Sion 1999), and SDSS J104559.13+590448.3, SDSS J104559.14+590448.3, and SDSS J104559.15+590448.2 (Abolfathi et al. 2018).

0.14 mas that can be directly converted to distance  $d = 57.2^{+0.4}_{-0.3}$  pc without significant loss of accuracy (Bailer-Jones et al. 2018; Luri et al. 2018). We may calculate the 3-D space motion for LP 93-21 by combining *Gaia*’s proper motion measurements and the SDSS radial velocity measurement. We include the radial velocity measurement from its SDSS spectrum of 462 km s<sup>-1</sup> (Kleinman et al. 2013) and add a conservative radial velocity error of  $\pm 20$  km s<sup>-1</sup>, which we assume is uncorrelated with the *Gaia* observables.

To integrate LP 93-21’s orbit, we used the `astropy` (Astropy Collaboration et al. 2013, 2018) affiliated `python` package `gala`<sup>2</sup> (Price-Whelan 2017). We chose the Milky Way potential in `gala` which assumes a mass-model containing a spherical nucleus and bulge based on the Hernquist potential for a spheroid (Hernquist 1990), a disk based on the Miyamoto-Nagai potential for a flattened mass distribution (Miyamoto & Nagai 1975), and a spherical NFW dark matter halo potential (Navarro et al. 1996). The relative weighting for each component is taken from (Bovy (2015); see their Table 1). We define the Sun’s position at  $x = -8.3$  kpc from the Galactic centre in the midplane ( $z = 0$ ) of the Milky Way, and use an upper-limit circular velocity estimate of 250 km s<sup>-1</sup> (Bovy et al. 2012; Eilers et al. 2019). We drew initial positions for each orbit from the observed covariance matrix, as described in Lindegren et al. (2018), which factors in the correlation between the *Gaia* observables.

We find LP 93-21 is currently travelling at approximately  $v_{\text{gal}} = 605$  km s<sup>-1</sup> with a local galactic escape speed of approximately  $v_{\text{esc}} = 557$  km s<sup>-1</sup>, making it locally unbound to the Milky Way’s gravitational potential. At a distance of  $d = 57.2^{+0.4}_{-0.3}$  pc, LP 93-21 is the closest hyper-runaway star to the Sun. Figure 1 shows LP 93-21’s integrated orbit forwards and backwards in time 250 Myr – approximately the timescale of one Solar orbit around the Galactic centre. For all 100 orbits drawn, LP 93-21 is unbound to the Milky Way’s gravitational potential. Figure 2 shows its proximity to the Sun. LP 93-21’s closest approach to the Sun would have been approximately 70,000 years ago at a distance of about 46 pc.

The observed velocity of LP 93-21 is currently being influenced by the Milky Way’s gravitational potential. By integrating LP 93-21’s orbit in `gala`, we take into account its velocity over time only as it has been affected by the Milky Way’s gravitational potential. If we consider an extragalactic origin for LP 93-21 then as it approached the disk of the Milky Way the gravitational pull began to accelerate it and increase its speed (see Figure 3, bottom right).

If LP 93-21 did have an extragalactic origin, then by integrating backwards we find that at a distance of approximately 100 kpc from the Galactic centre (taken as a proxy for the virial radius of the Milky Way), LP 93-21’s galactocentric velocity is about 400 km s<sup>-1</sup>. This would correspond to a flight time of about 220 Myr from a 100 kpc galactocentric radius to LP 93-21’s current position. This provides an upper limit for ejection time if the SN kick occurred within the Milky Way.

Based on kinematic information alone, we can exclude the Galactic centre as the origin of LP 93-21, as well as the Magellanic clouds, and six known supernova rem-

<sup>2</sup> <https://gala-astro.readthedocs.io/en/latest/index.html>

| Parameter                         | Symbol             | Value               | Units                | Source                           |
|-----------------------------------|--------------------|---------------------|----------------------|----------------------------------|
| Right Ascension                   | $\alpha$           | $161.49 \pm 0.08$   | deg                  | Gaia Collaboration et al. (2018) |
| Declination                       | $\delta$           | $59.07 \pm 0.10$    | deg                  | Gaia Collaboration et al. (2018) |
| Proper motion in Right Ascension  | $\mu_\alpha$       | $-1019.19 \pm 0.14$ | mas yr <sup>-1</sup> | Gaia Collaboration et al. (2018) |
| Proper motion in Declination      | $\mu_\delta$       | $-1462.53 \pm 0.17$ | mas yr <sup>-1</sup> | Gaia Collaboration et al. (2018) |
| Parallax                          | $\varpi$           | $17.48 \pm 0.14$    | mas                  | Gaia Collaboration et al. (2018) |
| Radial velocity                   | $v_{\text{rad}}$   | $462 \pm 20$        | km s <sup>-1</sup>   | Abolfathi et al. (2018)          |
| Apparent <i>G</i> -band magnitude | $G_{\text{app}}$   | 17.7                | mag                  | Gaia Collaboration et al. (2018) |
| Absolute <i>G</i> -band magnitude | $G_{\text{abs}}$   | 13.8                | mag                  | Gaia Collaboration et al. (2018) |
| <i>BP</i> – <i>RP</i> colour      | $C_{\text{bp-rp}}$ | 0.24                | mag                  | Gaia Collaboration et al. (2018) |
| Mass                              | $M$                | $1.029 \pm 0.015$   | $M_\odot$            | Kilic et al. (2018)              |
| Effective temperature             | $T_{\text{eff}}$   | $8690 \pm 120$      | K                    | Kilic et al. (2018)              |
| Surface gravity                   | log <i>g</i>       | $8.701 \pm 0.02$    | cm s <sup>-2</sup>   | Kilic et al. (2018)              |
| Carbon abundance                  | [C/He]             | -3.51               | dex                  | Kilic et al. (2018)              |
| White dwarf cooling age           | $t_{\text{WD}}$    | $2.715 \pm 0.08$    | Gyr                  | Kilic et al. (2018)              |

**Table 1.** Measured properties of LP 93-21.

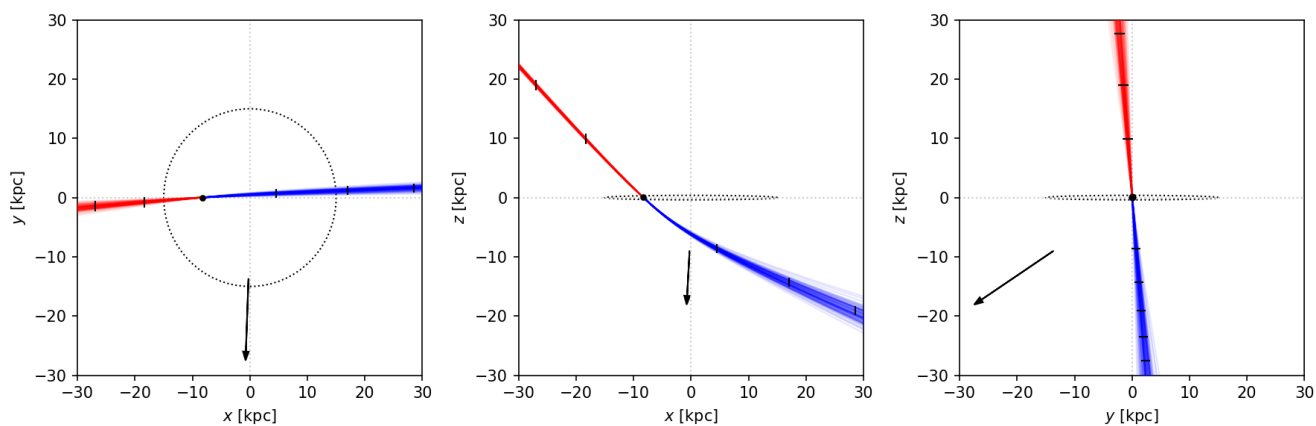


**Figure 1.** LP 93-21’s orbit. The current position of LP 93-21 is shown by a black circle. The integrated orbits trace LP 93-21’s movement forward in time (red) and backwards in time (blue). The spread in orbit directions is caused by the uncertainty in *Gaia* and SDSS measurements. The extent of the Milky Way’s spiral arms are approximated by the darker, dashed circle, and the galactic centre is approximated by the intersection of the lighter, dashed lines. The direction to the Large Magellanic Cloud is denoted by a black arrow. Each hash mark indicates approximately 25 million years of flight either forwards or backwards in time. Note LP 93-21 is unbound in all 100 integrated orbits.

nants (SN1006A, SN1054A, SN1604A, SN185A, SN393A, and Vela; Green (2014)). Figure 3 shows the kinematic and positional evolution for LP 93-21. The galactocentric  $z$ -coordinate  $Z_{\text{gal}}$ , galactocentric radius  $R_{\text{gal}}$ , and heliocentric distance  $d_{\text{helio}}$  all show asymptotic behavior, characteristic of unbound stars.

## 2.2 Current mass & age estimates

Kilic et al. (2018) identified 142 *Gaia* sources as halo WDs and presented detailed model atmosphere analysis for each one based on *Gaia* parallaxes and optical and near-infrared photometry. They used a pure helium atmosphere model with trace amounts of carbon to simultaneously fit the spectral energy distribution (SED) and the optical spectra for LP 93-21. The results of this fit are summarised in Table 1. Weidemann (2005) notes the inaccuracies of using He-dominated DB WD models as a replacement for DQ WDs without accounting for this enhanced carbon composition, implying that the detailed analysis by Kilic et al. (2018) is

the current state-of-the-art. LP 93-21’s mass is found to be  $1.03 M_\odot$ , making it a massive outlier in SDSS (Kepler et al. (2007); see their Figure 13). LP 93-21’s WD age is estimated by Kilic et al. (2018) to be 2.715 Gyr, under the assumption of zero mass transfer.

Leggett et al. (2018) presented new US Naval Observatory Flagstaff Station parallaxes for over 170 WDs. They combined recent *Gaia* parallaxes with photometry spanning from the mid-infrared to the ultraviolet to determine flux-calibrated SEDs for each WD. The SEDs were compared to flux distributions provided by various recent model atmospheres compiled by the authors. Leggett et al. (2018) demonstrate the models reproduce the full SED very well for the entire sample of WDs. LP 93-21’s mass is again found to be an outlier at  $1.14 M_\odot$ , and its WD age is estimated to be 2.366 Gyr, under the assumption of zero mass transfer.

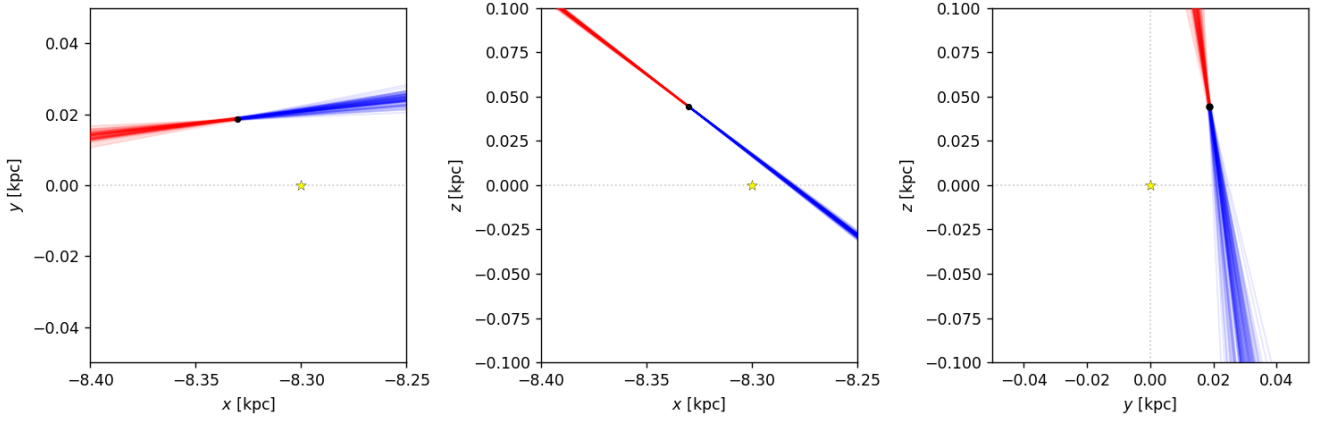


**Figure 2.** LP 93-21’s proximity to the Sun. The current position of LP 93-21 is shown by a black circle. The position of the Sun is denoted by a yellow star. The integrated orbits trace LP 93-21’s movement forward in time (red) and backwards in time (blue). The spread in orbit directions is caused by the uncertainty in *Gaia* and SDSS measurements. LP 93-21’s closest approach around 70,000 years ago was approximately 46 pc.

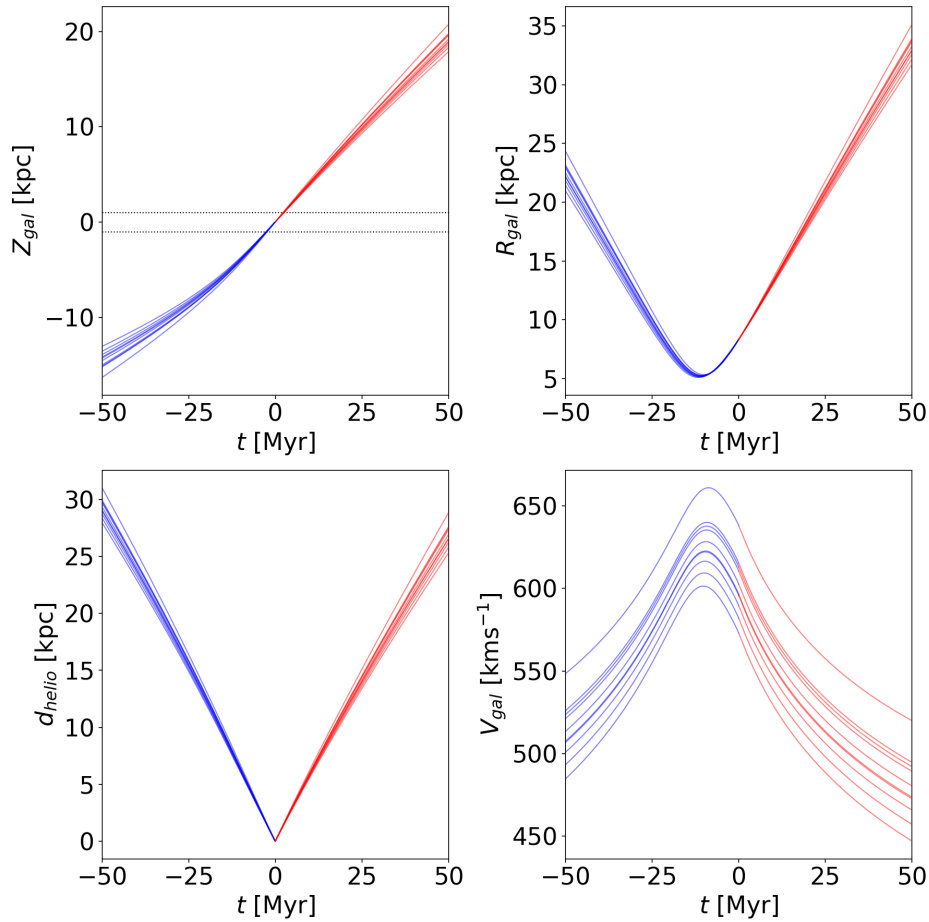


**Figure 3.** Kinematic and positional parameters for LP 93-21 shown as a function of flight time  $t$ . Movement forward in time is denoted in red and movement backwards in time is denoted in blue. Top left: galactocentric  $z$ -coordinate  $Z_{\text{gal}}$ . The vertical extent of the thick disk is approximated by the dashed lines. Top right: galactocentric radius  $R_{\text{gal}}$ . Bottom left: heliocentric distance  $d_{\text{helio}}$ . Bottom right: galactocentric rest-frame velocity  $v_{\text{gal}}$ .

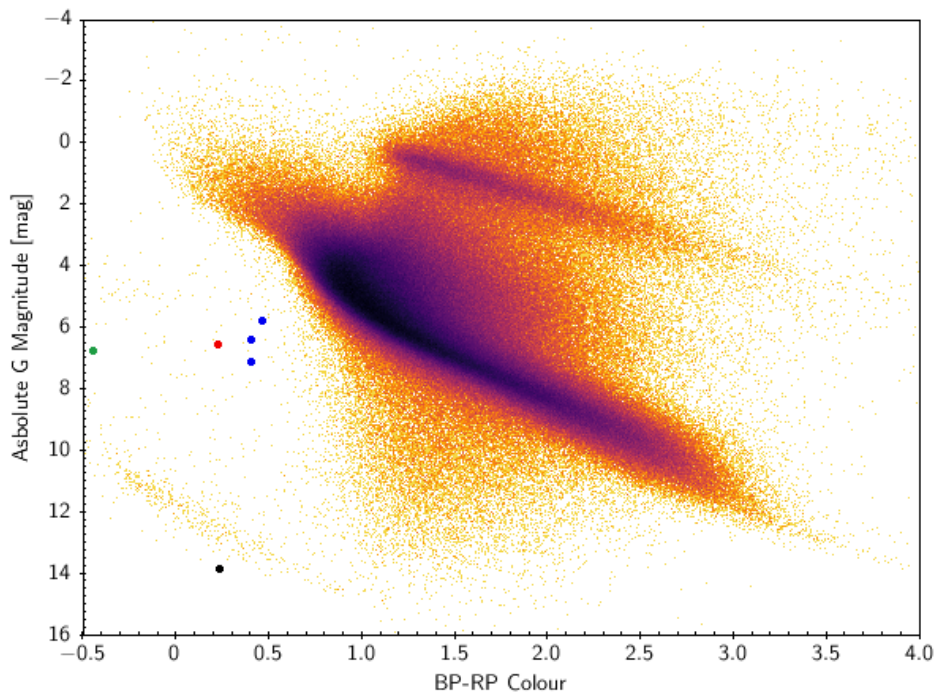


**Figure 4.** Hertzsprung-Russell diagram showing a random sample of one million *Gaia* stars with usual features such as the main sequence, giant branch, and white dwarf sequence. LP 93-21 is denoted by a black dot within the main white dwarf sequence at an approximate absolute *G*-band magnitude of 13.8 mag. Other known unbound WDs are shown. The three “D<sup>6</sup>” hyper-runaway WD candidates (Shen et al. 2018a) are denoted by blue dots. The hyper-runaway WD candidate LP 40-365 (Raddi et al. 2018) is denoted by a red dot. The hyper-runaway US 708 (Hirsch et al. 2005) is denoted by a green dot.

### 3 DISCUSSION

LP 93-21 is an exceptionally fast-moving WD, moving much quicker than would be expected for a normal, Milky Way halo WD (Oppenheimer et al. 2001; Bergeron 2003; Bergeron et al. 2005; Pauli et al. 2006; Ducourant et al. 2007). LP 93-21’s observed velocity likely excludes it from normal dynamical ejection from a globular cluster because simulations estimate that  $\approx 99\%$  of all dynamical ejections of this type have less than  $200 \text{ km s}^{-1}$  velocities (Perets & Šubr 2012). LP 93-21’s observed velocity also likely excludes it from the core-collapse binary supernova ejection scenario. Simulations estimate that only the fastest few percent of stars ejected via core-collapse supernovae reach speeds of over  $200 \text{ km s}^{-1}$  (Tauris 2015).

If LP 93-21 originates from the Milky Way, we find its velocity was very likely never below  $400 \text{ km s}^{-1}$ . Therefore, the mechanisms that may explain LP 93-21’s velocity (if from the Milky Way) include dynamical ejection from the Galactic centre or a binary SNe Ia/Iax ejection. Given LP 93-21 does not originate from the Galactic centre (or any other location where a central, massive black hole is expected to be, see Figure 1), and can be excluded from other dynamical scenarios based on its observed speed, the most plausible mechanism to describe its velocity is the SNe Ia/Iax ejection scenario.

The progenitor configuration most compatible with LP 93-21’s observed speed is the SD scenario proposed for SNe Ia/Iax between a primary WD and He-burning donor star (Wang & Han 2009; Wang et al. 2017; Wong & Schwab 2019; Bauer et al. 2019). In the SN Ia scenario, the primary WD reaches Chandrasekhar-mass through accretion,

explodes as a SN Ia, and the DR is ejected at roughly the pre-SN orbital velocity (Eldridge et al. 2011; Tauris 2015; Shen et al. 2018a). In the SN Iax scenario, ejection speeds on the order of a few tens to a few hundred  $\text{km s}^{-1}$  are expected for both the DR and PR, due to the expected asymmetric explosion and ejecta interaction (Jordan et al. 2012; Pan et al. 2012b,d; Liu et al. 2012, 2013b; Kromer et al. 2015).

It is unlikely that LP 93-21 was a WD while donating mass to its former primary companion in the DD scenario. Due to the relatively short upper-limit Milky Way flight time of 220 Myr for LP 93-21 (see Section 2.1), its maximum Milky Way speed was likely never above  $\approx 625 \text{ km s}^{-1}$  (see Figure 3). The expected tell-tale kinematic signature (i.e.  $> 1,000 \text{ km s}^{-1}$  in all cases) indicates LP 93-21 should still be possessing a much quicker total speed if it were ejected as a WD in the DD scenario (Shen et al. 2018a; Tanikawa et al. 2018). This is also indicated by Figure 1. If shot through the Milky Way’s disk with a characteristic speed of  $> 1,000 \text{ km s}^{-1}$ , LP 93-21 should have only been accelerated to quicker speeds after its ejection. Thus, the DD scenario is unlikely for LP 93-21 based on its observed speed alone.

The SD SN Ia scenario implies LP 93-21 was a mass-donating He-star companion that was ejected by the detonation of its primary<sup>3</sup>. In this scenario the relatively short upper-limit Milky Way flight time of 220 Myr for LP 93-21 (see Section 2.1), when combined with the updated WD cooling age estimates of over 2 Gyr from both Kilic et al. (2018) and Leggett et al. (2018), demands an origin from

<sup>3</sup> In the same way, the SN Iax scenario also implies LP 93-21 may have been a former He-star donor.

elsewhere than the Milky Way. LP 93-21 would have then evolved into a WD while travelling through inter-galactic space.

We find this scenario is an unlikely explanation for LP 93-21's origin because of the low probability that an extra-galactic hyper-runaway star would pass so close to the Sun. We took over 850 nearby galaxies from the Updated Nearby Galaxy Catalog (Karachentsev et al. 2013) and estimated SN Ia rates given the galaxy mass and rate-size relations from Li et al. (2011). We assume an average speed of  $600 \text{ km s}^{-1}$ , which assumes some deceleration as the DR escapes the gravitational potential of the host galaxy and acceleration as the DR approaches the Milky Way. If we assume that the DRs are ejected in isotropic directions and that a fully-cooled down DR could be observed by *Gaia* out to a distance of 100 pc, then the expected number of observable DRs from a the  $n$ th galaxy is given by the ratio of observable volume to the volume of a sphere with a radius equal to the galaxy's distance

$$E_n = \left( \frac{100 \text{ pc}}{d_n} \right)^3 \text{SNuM}(M_n) \Delta t \quad (1)$$

where  $d_n$  is the distance to the host galaxy, and  $\text{SNuM}(M_n)$  is the SN Ia rate as a function of galaxy mass. Here  $\Delta t$  is conservatively taken as the maximum time the DR could take to pass through the observable volume: the time taken for DR to travel twice the observable radius (towards and away from us;  $\Delta t = 2 \frac{100 \text{ pc}}{600 \text{ km s}^{-1}} \approx 3.3 \times 10^6 \text{ yr}$ ). After summing the expected number of observable DRs from all nearby galaxies we find that only  $10^{-4}$  of fully-cooled, extra-galactic DRs would be expected. This value remains much less than one even if we relax our assumptions. This low expectation value indicates it is highly unlikely any extra-galactic DR is within 100 pc of the Sun, including LP 93-21.

If ejected as a He-star, a corresponding rotation speed and detailed elemental abundances would be paramount in determining the viability of this scenario for LP 93-21. It is expected that LP 93-21 would be a very fast rotator, and that a nontrivial abundance of decayed nickel might still be visible on its surface (Fuller & Lai 2012; Pan et al. 2012b; Liu et al. 2013a). Trace amounts of intermediate-mass elements might also point to the He-star SD SN Ia channel as the explanation for LP 93-21's observed speed (Pan et al. 2012d; Liu et al. 2013b).

Conversely, the SN Iax explanation implies LP 93-21 was possibly a former *primary* WD in the same SD configuration between a WD and companion He-star. The upper-limit Milky Way flight time is now consistent with its WD cooling age, by this explanation. Primary WDs which have possibly survived their own partial deflagrations make a new class of stars based on distinct kinematic and abundance signatures (Raddi et al. 2019). The observed speeds of these objects agree well with LP 93-21's. But as shown by the red dot in Figure 4, these objects do not appear as ordinary WDs. The handful of objects found appear to be ‘‘puffed-up’’ WDs, meaning they are brighter and slightly red-shifted when compared to normal WDs (see Figure 4 and Raddi et al. (2019)). The degeneracy in their cores may have been lifted slightly due to the deflagration and accretion of ejecta (Shen et al. 2018a; Raddi et al. 2019).

Simulations of WDs which include radiative levitation and gravitational settling suggest that the observable effects

from the deflagration should dissipate over relatively short timescales for the primary WD, but that a second heating and brightening phase could last on the order of 10 Myr until these objects eventually evolve back to the canonical WD cooling sequence (Zhang et al. 2019). The current location of LP 40-365 is therefore likely temporary, as the direct visual effects dissipate much sooner than a typical Galactic crossing time for an unbound PR (about 100–150 Myr, Raddi et al. (2018)).

Due to its position in Figure 4, LP 93-21 could represent the first fully ‘‘cooled-down’’ PR observed in this new class of stars similar to LP 40-365 (Zhang et al. 2019; Bauer et al. 2019). LP 93-21's enhanced C abundance agrees well with this scenario, although its bulk composition may not fully reflect in surface abundances (Zhang et al. 2019). Carbon burning is required in Iax deflagrations, but incomplete in such explosions, so PRs are likely to have substantial carbon abundances (Zhang et al. 2019). LP 93-21 is a massive WD outlier ( $> 1.0 M_{\odot}$ ), and three-dimensional hydrodynamic simulations suggest that pure deflagrations of hybrid C/O/Ne WDs may leave massive bound remnants, which is inconsistent with the observed stars like LP 40-365 ( $\approx 0.2\text{--}0.3 M_{\odot}$ ) which were likely left by pure deflagrations of C/O or O/Ne WDs (Kromer et al. 2015; Raddi et al. 2019).

## 4 CONCLUSIONS

Using *Gaia* DR2, we were able to confirm LP 93-21 exhibits a total space velocity of approximately  $v_{\text{gal}} = 605 \text{ km s}^{-1}$ , with a local galactic escape speed of approximately  $v_{\text{esc}} = 557 \text{ km s}^{-1}$ . We found its orbit to be unbound to the Milky Way in all cases. LP 93-21's orbit implies that it has travelled at most 220 Myr if originating from the Milky Way. The SN Iax-ejection scenario is consistent with its observed velocity, and a detailed spectrum may confirm if LP 93-21's own partial deflagration in a SN Iax caused such an ejection from the Milky Way.

If a portion of SNe Ia/Iax progenitors are a result of the He-star donor channel, the post-explosion kinematics necessarily produces a population of single WDs with high velocities, possibly containing distinguishing elemental abundances (Wang & Han 2009; Liu et al. 2018; Wang 2018; Zhang et al. 2019; Raddi et al. 2019). Thus it is possible that many high-velocity, slightly evolved He-stars and high-velocity WD remnants originate from both the SN Ia and SN Iax progenitor channels.

However, WDs are intrinsically very faint, so magnitude-limited surveys have historically had difficulties finding representative populations for WD analysis outside the Solar neighbourhood. LP 93-21's chance proximity to the Sun enabled discovery and observations easier than most for the likely numerous WD remnants kicked in the SNe Ia/Iax scenarios. In the future, magnitude-limited surveys should improve for very faint magnitudes and many more ‘‘cooled-down’’ remnants of these scenarios are likely to be found.

Regardless of the origin, LP 93-21 is the closest hyper-runaway WD candidate to the Sun. Other SNe Ia/Iax progenitor remnant candidates are shown on a Hertzsprung-Russel diagram of BP-RP colour versus absolute  $G$ -band magnitude in Figure 4. In four cases, a detailed spectral

analysis was used in conjunction with a kinematic analysis to constrain the nature of the progenitor systems that likely caused their high velocities. All four candidates were WDs found to be enhanced in key elements and unbound to the Milky Way’s gravitational potential. Due to the scarcity of known objects of this type, it is possible that LP 93-21 is the first identified example of a fast-moving, “cooled down” primary remnant and could represent a missing piece of the SNe Ia/Iax-ejected WD cooling sequence.

Further spectral analysis would provide constraints on the viability of the SNe Ia/Iax scenario in explaining LP 93-21’s observed speed. A detailed spectrum would allow measurements of LP 93-21’s spin and of key elemental abundances that might or might not still be on its surface. More surviving remnants are likely contained within the *Gaia* data and still need to be found throughout the Milky Way, waiting to help shed light on the SNe Ia/Iax progenitor problem.

## ACKNOWLEDGEMENTS

The authors would like to thank the anonymous referee for a detailed review, as well as Morgan Fraser (University College Dublin), Alexander Heger (Monash University), Adrian Price-Whelan (Princeton), Amanda Karakas (Monash University), Tin Long Sunny Wong (University of California Santa Cruz), and Paul Canton (University of Oklahoma) for useful conversations. A. R. C. is supported by the Australian Research Council (ARC) through Discovery Project DP160100637.

This research has made use of NASA’s Astrophysics Data System (<https://ui.adsabs.harvard.edu/>). This research has made use of the following software: `astropy`, a community-developed core Python package for astronomy (Astropy Collaboration et al. 2013, 2018), `TOPCAT` (Taylor 2005), `gala` (Price-Whelan 2017), `numpy` (Van Der Walt et al. 2011), and `matplotlib` (Hunter 2007).

This work has made use of CosmoHub (Carretero et al. 2017). CosmoHub has been developed by the Port d’Informació Científica (PIC), maintained through a collaboration of the Institut de Física d’Altes Energies (IFAE) and the Centro de Investigaciones Energéticas, Medioambientales y Tecnológicas (CIEMAT), and was partially funded by the “Plan Estatal de Investigación Científica y Técnica y de Innovación” program of the Spanish government.

This work has made use of data from the European Space Agency (ESA) mission *Gaia* (<https://www.cosmos.esa.int/gaia>), processed by the *Gaia* Data Processing and Analysis Consortium (DPAC, <https://www.cosmos.esa.int/web/gaia/dpac/consortium>). Funding for the DPAC has been provided by national institutions, in particular the institutions participating in the *Gaia* Multilateral Agreement.

This research has made use of data from the Sloan Digital Sky Survey (<https://www.sdss.org/>). Funding for the Sloan Digital Sky Survey IV has been provided by the Alfred P. Sloan Foundation, the U.S. Department of Energy Office of Science, and the Participating Institutions. SDSS-IV acknowledges support and resources from the Center for High-Performance Computing at the University of Utah. The SDSS web site is [www.sdss.org](http://www.sdss.org).

SDSS-IV is managed by the Astrophysical Research Consortium for the Participating Institutions of the SDSS Collaboration including the Brazilian Participation Group, the Carnegie Institution for Science, Carnegie Mellon University, the Chilean Participation Group, the French Participation Group, Harvard-Smithsonian Center for Astrophysics, Instituto de Astrofísica de Canarias, The Johns Hopkins University, Kavli Institute for the Physics and Mathematics of the Universe (IPMU) / University of Tokyo, the Korean Participation Group, Lawrence Berkeley National Laboratory, Leibniz Institut für Astrophysik Potsdam (AIP), Max-Planck-Institut für Astronomie (MPIA Heidelberg), Max-Planck-Institut für Astrophysik (MPA Garching), Max-Planck-Institut für Extraterrestrische Physik (MPE), National Astronomical Observatories of China, New Mexico State University, New York University, University of Notre Dame, Observatório Nacional / MCTI, The Ohio State University, Pennsylvania State University, Shanghai Astronomical Observatory, United Kingdom Participation Group, Universidad Nacional Autónoma de México, University of Arizona, University of Colorado Boulder, University of Oxford, University of Portsmouth, University of Utah, University of Virginia, University of Washington, University of Wisconsin, Vanderbilt University, and Yale University.

## REFERENCES

- Abolfathi B., et al., 2018, *ApJS*, **235**, 42  
 Astropy Collaboration et al., 2013, *A&A*, **558**, A33  
 Astropy Collaboration et al., 2018, *AJ*, **156**, 123  
 Bailer-Jones C. A. L., Rybizki J., Fouesneau M., Mantelet G., Andrae R., 2018, *AJ*, **156**, 58  
 Bauer E. B., White C. J., Bildsten L., 2019, arXiv e-prints, p. [arXiv:1906.08941](https://arxiv.org/abs/1906.08941)  
 Bergeron P., 2003, *ApJ*, **586**, 201  
 Bergeron P., Ruiz M. T., Hamuy M., Leggett S. K., Currie M. J., Lajoie C. P., Dufour P., 2005, *ApJ*, **625**, 838  
 Blanton M. R., et al., 2017, *AJ*, **154**, 28  
 Bovy J., 2015, *The Astrophysical Journal Supplement Series*, **216**, 29  
 Bovy J., et al., 2012, *ApJ*, **759**, 131  
 Carretero J., et al., 2017, in Proceedings of the European Physical Society Conference on High Energy Physics. 5-12 July. p. 488  
 Ducourant C., Teixeira R., Hambly N. C., Oppenheimer B. R., Hawkins M. R. S., Rapaport M., Modolo J., Lecampion J. F., 2007, *A&A*, **470**, 387  
 Eilers A.-C., Hogg D. W., Rix H.-W., Ness M. K., 2019, *ApJ*, **871**, 120  
 Eldridge J. J., Langer N., Tout C. A., 2011, *MNRAS*, **414**, 3501  
 Fink M., et al., 2014, *MNRAS*, **438**, 1762  
 Foley R. J., et al., 2013, *ApJ*, **767**, 57  
 Fuller J., Lai D., 2012, *MNRAS*, **421**, 426  
 Gaia Collaboration et al., 2016, *A&A*, **595**, A1  
 Gaia Collaboration et al., 2018, *A&A*, **616**, A1  
 Green D. A., 2014, Bulletin of the Astronomical Society of India, **42**, 47  
 Greenstein J. L., Oke J. B., Richstone D., van Altena W. F., Steppe H., 1977, *ApJ*, **218**, L21  
 Hansen B. M. S., 2003, *The Astrophysical Journal*, **582**, 915  
 Hernquist L., 1990, *ApJ*, **356**, 359  
 Hirsch H. A., Heber U., O’Toole S. J., Bresolin F., 2005, *A&A*, **444**, L61  
 Hunter J. D., 2007, *Computing in Science and Engineering*, **9**, 90  
 Iben I. J., Tutukov A. V., 1984, *The Astrophysical Journal Supplement Series*, **54**, 335

- Iben Icko J., Tutukov A. V., 1994, *ApJ*, **431**, 264
- Jordan George C. I., Perets H. B., Fisher R. T., van Rossum D. R., 2012, *ApJ*, **761**, L23
- Justham S., Wolf C., Podsiadlowski P., Han Z., 2009, *A&A*, **493**, 1081
- Karachentsev I. D., Makarov D. I., Kaisina E. I., 2013, *AJ*, **145**, 101
- Kepler S. O., Kleinman S. J., Nitta A., Koester D., Castanheira B. G., Giovannini O., Costa A. F. M., Althaus L., 2007, *MNRAS*, **375**, 1315
- Kilic M., Bergeron P., Dame K., Hambly N. C., Rowell N., Crawford C. L., 2018, preprint, p. [arXiv:1810.03536](https://arxiv.org/abs/1810.03536) ([arXiv:1810.03536](https://arxiv.org/abs/1810.03536))
- Kleinman S. J., et al., 2013, *The Astrophysical Journal Supplement Series*, **204**, 5
- Kromer M., et al., 2013, *MNRAS*, **429**, 2287
- Kromer M., et al., 2015, *MNRAS*, **450**, 3045
- Leggett S. K., et al., 2018, *ApJS*, **239**, 26
- Li W., Chornock R., Leaman J., Filippenko A. V., Poznanski D., Wang X., Ganeshalingam M., Mannucci F., 2011, *MNRAS*, **412**, 1473
- Lindgren L., et al., 2018, *A&A*, **616**, A2
- Liu Z. W., Pakmor R., Röpke F. K., Edelmann P., Wang B., Kromer M., Hillebrandt W., Han Z. W., 2012, *A&A*, **548**, A2
- Liu Z. W., Pakmor R., Röpke F. K., Edelmann P., Hillebrandt W., Kerzendorf W. E., Wang B., Han Z. W., 2013a, *A&A*, **554**, A109
- Liu Z.-W., et al., 2013b, *ApJ*, **774**, 37
- Liu D., Wang B., Han Z., 2018, *MNRAS*, **473**, 5352
- Luri X., et al., 2018, *A&A*, **616**, A9
- Luyten W. J., 1976, Univ. Minnesota, p. 0
- McCook G. P., Sion E. M., 1999, *The Astrophysical Journal Supplement Series*, **121**, 1
- Miyamoto M., Nagai R., 1975, *PASJ*, **27**, 533
- Navarro J. F., Frenk C. S., White S. D. M., 1996, *ApJ*, **462**, 563
- Nomoto K., 1982, *ApJ*, **253**, 798
- Nomoto K., Iwamoto K., Kishimoto N., 1997, *Science*, **276**, 1378
- Oppenheimer B. R., Hambly N. C., Digby A. P., Hodgkin S. T., Saumon D., 2001, *Science*, **292**, 698
- Pakmor R., Kromer M., Taubenberger S., Sim S. A., Röpke F. K., Hillebrandt W., 2012, *ApJ*, **747**, L10
- Pan K.-C., Ricker P. M., Taam R. E., 2012a, *ApJ*, **750**, 151
- Pan K.-C., Ricker P. M., Taam R. E., 2012b, *ApJ*, **750**, 151
- Pan K.-C., Ricker P. M., Taam R. E., 2012c, *ApJ*, **760**, 21
- Pan K.-C., Ricker P. M., Taam R. E., 2012d, *ApJ*, **760**, 21
- Papish O., Soker N., García-Berro E., Aznar-Siguán G., 2015, *MNRAS*, **449**, 942
- Pauli E. M., Napiwotzki R., Heber U., Altmann M., Odenkirchen M., 2006, *A&A*, **447**, 173
- Perets H. B., Šubr L., 2012, *ApJ*, **751**, 133
- Perlmutter S., et al., 1999, *ApJ*, **517**, 565
- Price-Whelan A. M., 2017, *The Journal of Open Source Software*, **2**, 388
- Raddi R., Hollands M. A., Gänsicke B. T., Townsley D. M., Hermes J. J., Gentile Fusillo N. P., Koester D., 2018, *MNRAS*, **479**, L96
- Raddi R., et al., 2019, arXiv e-prints, p. [arXiv:1902.05061](https://arxiv.org/abs/1902.05061)
- Riess A. G., et al., 1998, *AJ*, **116**, 1009
- Seitenzahl I. R., Cescutti G., Röpke F. K., Ruiter A. J., Pakmor R., 2013, *A&A*, **559**, L5
- Shen K. J., Schwab J., 2017, *ApJ*, **834**, 180
- Shen K. J., et al., 2018a, preprint, p. [arXiv:1804.11163](https://arxiv.org/abs/1804.11163) ([arXiv:1804.11163](https://arxiv.org/abs/1804.11163))
- Shen K. J., Kasen D., Miles B. J., Townsley D. M., 2018b, *ApJ*, **854**, 52
- Tanikawa A., Nomoto K., Nakasato N., 2018, *ApJ*, **868**, 90
- Tauris T. M., 2015, *MNRAS*, **448**, L6
- Taylor M. B., 2005, in Shopbell P., Britton M., Ebert R., eds, *Astronomical Society of the Pacific Conference Series Vol. 347, Astronomical Data Analysis Software and Systems XIV*. p. 29
- Van Der Walt S., Colbert S. C., Varoquaux G., 2011, preprint, p. [arXiv:1102.1523](https://arxiv.org/abs/1102.1523) ([arXiv:1102.1523](https://arxiv.org/abs/1102.1523))
- Wang B., 2018, *Research in Astronomy and Astrophysics*, **18**, 049
- Wang B., Han Z., 2009, *A&A*, **508**, L27
- Wang B., Han Z., 2010, *A&A*, **515**, A88
- Wang B., Han Z., 2011, preprint, p. [arXiv:1111.1503](https://arxiv.org/abs/1111.1503) ([arXiv:1111.1503](https://arxiv.org/abs/1111.1503))
- Wang B., Han Z., 2012, *New Astronomy Reviews*, **56**, 122
- Wang B., Podsiadlowski P., Han Z., 2017, *MNRAS*, **472**, 1593
- Webbink R. F., 1984, *ApJ*, **277**, 355
- Weidemann V., 2005, in Koester D., Moehler S., eds, *Astronomical Society of the Pacific Conference Series Vol. 334, 14th European Workshop on White Dwarfs*. p. 15
- Whelan J., Iben Icko J., 1973, *ApJ*, **186**, 1007
- Wong T. L. S., Schwab J., 2019, arXiv e-prints, p. [arXiv:1901.04512](https://arxiv.org/abs/1901.04512)
- Zhang M., Fuller J., Schwab J., Foley R. J., 2019, *ApJ*, **872**, 29

This paper has been typeset from a  $\text{\TeX}/\text{\LaTeX}$  file prepared by the author.